Pergamon

*Journal of Structural Geology*, Vol. 18, No. 5, pp. 573 to 583, 1996

0191-8141/96 $15.00+0.00

0191-8141(95)00133-6

# The use of finite strain data in constructing a retrodeformable cross-section of the Meade thrust sheet, southeastern Idaho, U.S.A.

MARK A. McNAUGHT* and GAUTAM MITRA

Department of Geological Sciences, University of Rochester, Rochester, NY 14627, U.S.A.

(*Received* 15 *February* 1995; *accepted in revised form* 20 *October* 1995)

**Abstract**—A method for drawing a balanced cross-section is presented which uses the constraint of both the interpretation of the geometry and the analysis of the internal deformation within the Meade thrust sheet, southeastern Idaho, U.S.A.

Earliest deformation associated with the Meade thrust sheet is layer-parallel shortening, which is indicated by a spaced solution cleavage and deformed fossils in the Jurassic Twin Creek Formation. This early layer-parallel shortening fabric is rotated by folding in front of the main Meade thrust sheet. These folds are then truncated by the Meade thrust. Locally, finite strain markers indicate fault-parallel shear. Copyright © 1996 Elsevier Science Ltd

## INTRODUCTION

Balanced and restorable cross-sections are powerful tools in understanding the development of fold and thrust belts. Balancing techniques were originally developed to constrain the possible geometries in the external part of a thrust belt, by assuming that either the length or the area of individual beds in the plane of section is conserved between the deformed section and the undeformed section (Woodward *et al.* 1985). Assumed deformation within any individual thrust sheet is limited to flexural-slip for line-length balancing or plane strain for area balancing when dealing with a two-dimensional cross-section. While such assumptions may be valid for the external portion of a fold and thrust belt, they clearly break down in internal thrust sheets where beds are penetratively deformed. Because of this, it is impossible to constrain the structural geometry without detailed knowledge of the deformation that has occurred within each unit. Even when detailed information is available, using the information to construct a restored section is not simple without knowledge of the deformation path.

Determination of the deformation path generally requires well-developed incremental strain markers. However, such markers are not always available. In this paper we restrict ourselves to the case where there are finite strain markers but no incremental strain markers. Since the deformation path cannot be exactly determined, a model path is substituted. This model path is developed using the relative timing of observed small-scale structures and invoking processes known to be active in this portion of the thrust belt such as layer-parallel shorting (LPS), fault-parallel shear and flexural-slip (Mitra & Yonkee 1985, Protzman & Mitra 1990). This model can be applied in the reverse order to a cross-section to test if a viable (Elliott 1983) restored section can be produced. If the restoration is successful, we refer to the section as being retrodeformable, but only in terms of the specified deformational model. If the section cannot be restored, then the cross-section or the deformation model must be altered and the retrodeformation process repeated.

In order to test this method, we have chosen a thrust sheet located at the transition between the internal portion of the fold-and-thrust belt (where thrusts carry basement and show strong penetrative deformation) and its external portion (where thrust sheets show little or no penetrative deformation). We classify this sheet as being transitional because it is penetratively deformed (i.e. spaced solution cleavage in micritic limestones, deformed fossils and oolites in other carbonate units) although the deformation is not very strong (<20% shortening). It is important to note that the label of a transitional sheet may be as dependent on lithology as on location: a thrust sheet carrying carbonate units may show more penetrative deformation than a thrust sheet in the same location composed of siliciclastics.

## REGIONAL GEOLOGY

The Idaho–Utah–Wyoming thrust belt is part of the Sevier orogenic belt in the North American Cordillera. A series of W-dipping thrust faults transported parts of the pre-existing Paleozoic and early Mesozoic miogeocline eastward during the late Cretaceous and early Tertiary Sevier orogeny (Armstrong & Oriel 1965) (Fig. 1). Seven major thrusts make up the Idaho–Wyoming–Utah salient of the Sevier thrust belt. From west to east they are the Willard, Paris, Meade, Crawford, Absaroka, Darby and Prospect thrusts (Fig. 1). The timing of movement of these thrusts is known from cross-cutting relationships and synorogenic conglomerates (Armstrong & Oriel 1965, Oriel & Armstrong 1966, Royse *et*

*Present address: Department of Geology, Layfayette College, Easton, PA 18042, U.S.A.

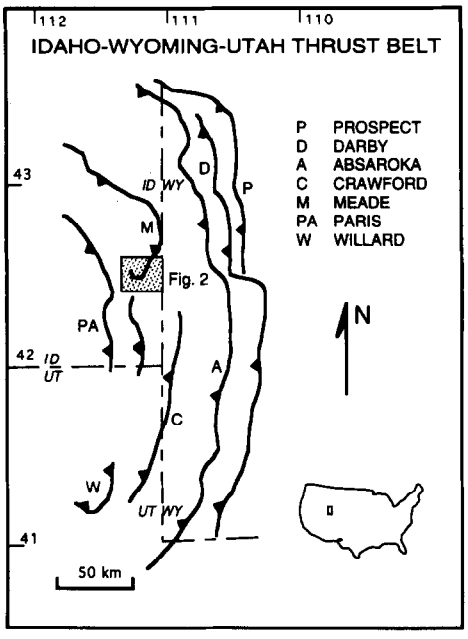


Fig. 1. Location of the study area and major thrust faults in the Idaho–Wyoming–Utah thrust belt of the western United States.

*al.* 1975, Wiltschko & Dorr 1983, Heller *et al.* 1986, DeCelles 1988). These dates indicate that the westernmost thrusts, the Willard and Paris, started to move first; movement proceeded sequentially eastward, although the oldest thrusts continued to be reactivated through the entire period of thrusting (DeCelles 1994).

The structures of the Idaho–Wyoming–Utah thrust belt are, in general, typical of the 'foothills family of structures' (Dahlstrom 1970). Major thrust faults are listric in shape and are asymptotic at depth with a low angle décollement (Royse *et al.* 1975, Dixon 1982, Lamerson 1982). This detachment is within the Cambrian section in the eastern external part of the thrust belt and drops into the Precambrian section toward the west (internal part). Although the overall shape of major thrusts are listric, in detail they have a ramp–flat geometry. Flats represent preferred glide horizons which a number of workers have demonstrated are stratigraphically controlled (Royse *et al.* 1975, Coogan & Yonkee 1985). Large-scale folding in the thrust belt is the result of movement of hanging wall ramps onto footwall flats and of folding at fault tip lines (fault-propagation folding) (McNaught & Mitra 1993). Smaller scale folds develop above imbricate fans that occur along some of the major thrusts. Normal faults bound many of the large, strike-parallel valleys in the thrust belts. These faults are listric in shape, joining with pre-existing thrusts at depth. Further west, normal faults become more common but their relationship to thrust belt structures is less clear (Royse *et al.* 1975, Burgel *et al.* 1987).

## THE MEADE THRUST

The Meade thrust is one of the major thrusts of the Idaho–Wyoming–Utah thrust belt. Its surface trace extends from the Snake River Plain in the north (Allmendinger 1981) to at least northernmost Utah (Blackstone & DeBruin 1987) in the south, and perhaps further (Valenti 1982, Dover 1985) (Fig. 1). Movement on the Meade thrust is dated as Late–Early Cretaceous (DeCelles *et al.* 1993). The Meade thrust is known to be younger than the Paris thrust to the west and older than the Crawford thrust to the east (Armstrong & Oriel 1965, Oriel & Armstrong 1966, Wiltschko & Dorr 1983, Mitra & Yonkee 1985).

This study was conducted about 15 km north of Montpelier, Idaho, where a sharp bend in the trace of the Meade thrust (Fig. 2) results from folding of the thrust sheet by younger imbricate thrusts (Coogan & Yonkee 1985). This folding allows both the hanging wall and footwall structure of the Meade thrust to be observed. This region along the Meade thrust has been studied by a number of workers (Mansfield 1927, Armstrong & Cressman 1963, Cressman 1964, Mitra & Yonkee 1985, Borden 1986, McNaught 1990, Protzman & Mitra 1990, Coogan & Royse 1990). In this area the Meade thrust places Mississippian-aged strata on Jurassic strata (Fig. 2). In the western part of the study area there is a hanging wall flat in the Mississippian section, above which a series of detachment folds comprise the major anticlines within the thrust sheet. The Snowdrift Mountain anticline, the easternmost of these folds, marks the hanging wall cut-off of the Mississippian section. East of this hanging wall cut-off, the Meade thrust splays into a series of imbricate thrusts that form two major imbricate slices (Fig. 2). The western slice contains an upright section ranging from Pennsylvanian to Triassic in age. The eastern slice contains an overturned section of Triassic and Jurassic strata. The oldest formation in the eastern slice, the Triassic Ankareh Formation, is also the youngest formation in the western slice. Both major slices are cut up by smaller imbricate faults (Fig. 2).

In the footwall, a series of anticlines are truncated by the Meade thrust (Fig. 2) (Protzman & Mitra 1990). For most of these footwall anticlines the thrust cuts only the Jurassic section. In the east limb of the westernmost Home Canyon anticline the thrust cuts overturned beds of Jurassic and part of the Triassic section, down to the Ankareh Formation, as seen in the northwest part of Fig. 2. Younger normal faults obscure the relationship between the west limb of the Home Canyon anticline and the Meade thrust. Traditionally the east limb of the Home Canyon anticline has been regarded as a footwall ramp of the Meade thrust which was folded above the Home Canyon thrust (Protzman & Mitra 1990). Recent work suggests a more complex structure in this region. Borden (1986) recognized that horses below the Meade thrust place upright Jurassic strata on the overturned Triassic and Jurassic strata that make up the footwall ramp (Fig. 2). This younger on older fault requires that the Meade thrust cut up- and down-section to the west.

Coogan & Royse (1990) also suggest that the Meade thrust cuts up- and down-section in this area because the

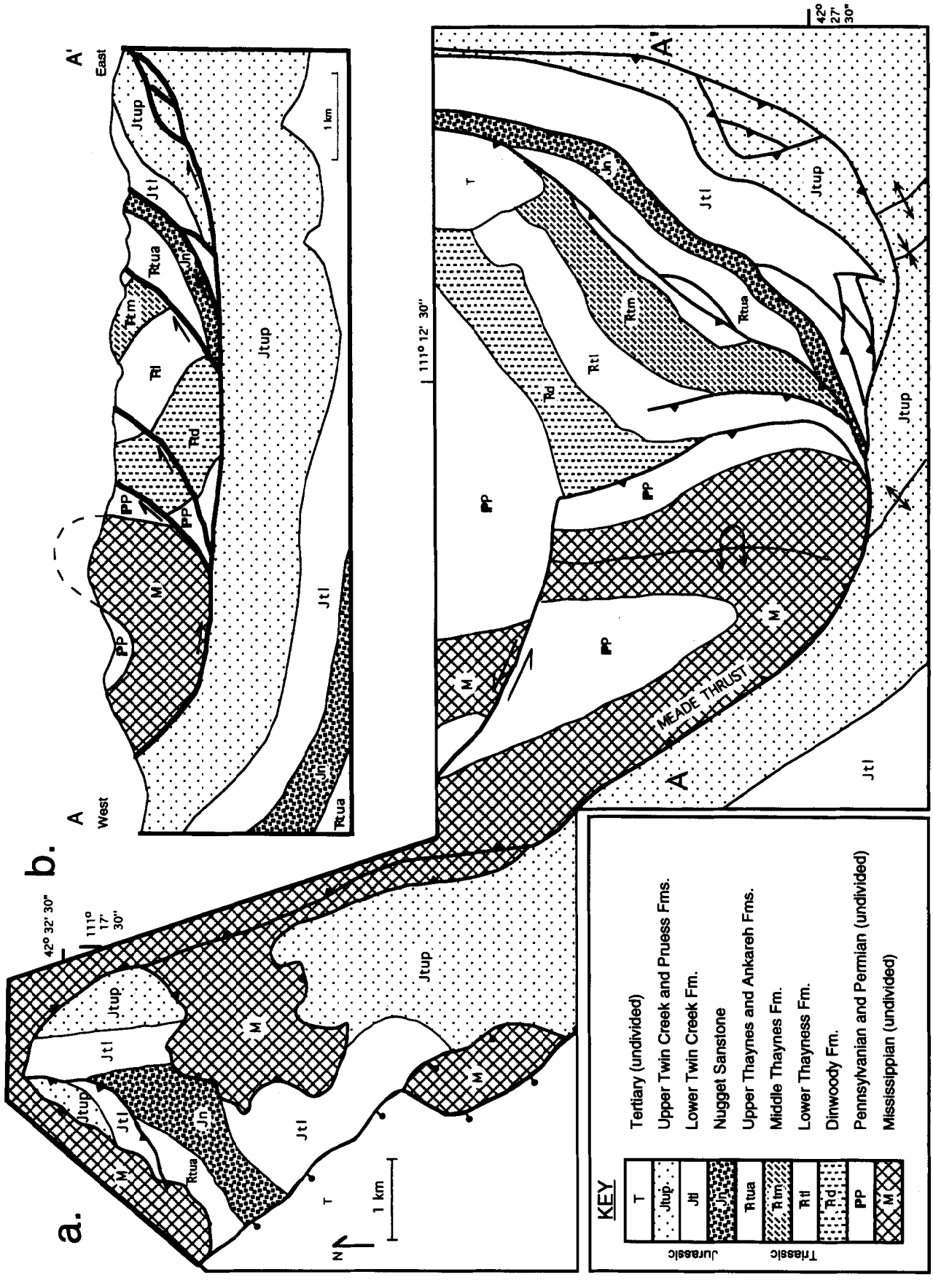


Fig. 2. (a) Geological map of the Meade Peak–Georgetown Canyon area. Line of cross-section A–A' is shown. Faults and folds are shown by standard symbols. Triangles mark hanging wall of thrust faults; ball and stick barbs mark hanging wall of normal faults. (b) Cross-section of the Meade Peak area along line A–A' in (a). Horizontal scale = vertical scale.

Union Texas Big Canyon Well penetrated Jurassic strata beneath the Meade thrust. This well, located 9 km northwest of the study area, is west of the apparent Jurassic footwall cut-off. Coogan & Royse (1990, fig. 17) suggest that the Meade thrust truncates the Home Canyon anticline as it does the other footwall anticlines further to the east (Protzman & Mitra 1990, fig. 2). They explain the apparent paradox of having a thrust cut, and be folded by, the same fold by having the thrust first truncate an earlier fold, and later be folded above a lower thrust. Allmendinger (1981) also suggested that the Meade thrust truncates folds in the hanging wall further to the north.

Our current interpretation for emplacement of the Meade thrust sheet in this area has detachment folds developing above the hanging wall imbricates of the Meade thrust (McNaught & Mitra 1993, fig. 2) as it steps up from a flat in the Triassic section to a flat in the Jurassic section. As the part of the Meade thrust sheet that carries the upper Paleozoic section overrides these detachment folds, imbricate faults cut up the folded strata into fault-bounded slices. These slices are transported various distances by the Meade thrust.

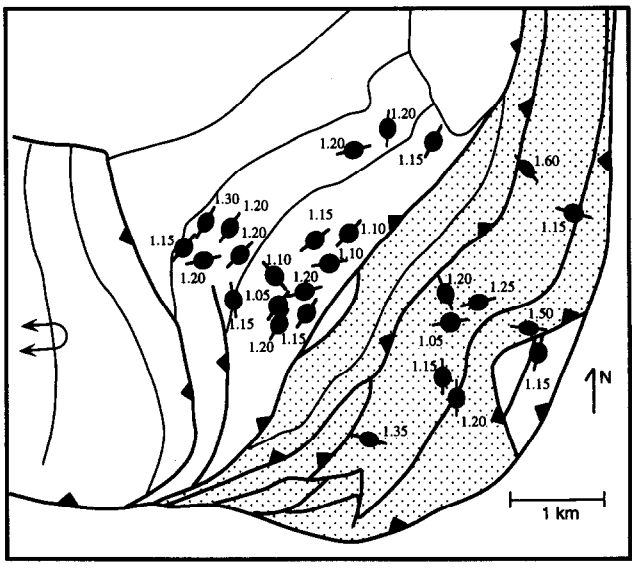


Fig. 3. Map of the Meade Peak area (southeastern part of Fig. 2a) showing the orientation of bedding plane strain ellipses determined from deformed *Pentacrinus* ossicles. Numbers indicate axial ratios. Stippled area marks overturned strata of eastern imbricate slice.

## STRAIN ANALYSIS

The Jurassic Twin Creek Formation, which is exposed in both the hanging wall to the east and the footwall to the west, is strongly deformed. A spaced cleavage is developed in the micritic units of the formation, not only in the Meade sheet but throughout the Idaho–Wyoming–Utah thrust belt, and has been extensively studied (Mitra *et al.* 1984, Mitra & Yonkee 1985). This cleavage is characterized by partings that develop along parallel seams of concentrated insolubles (quartz, potassium feldspar and clays) that developed owing to the localized removal of calcite by pressure solution (Mitra & Yonkee 1985). In the field, cleavage in the Twin Creek Formation is usually oriented at a high angle to bedding, is axial planar to early small-scale folds, and fans around later-formed large scale-folds remaining at a high angle to bedding and striking parallel to the trends of regional folds and the strike of regional thrusts (Mitra *et al.* 1988). Based on these field relationships, the cleavage is attributed to early layer parallel shortening (Mitra & Yonkee 1985, Mitra *et al.* 1988).

Finite strains (based on deformed fossils found primarily in a single fossil hash layer in the Leeds Creek member of the Jurassic Twin Creek Formation) in the footwall and frontal hanging wall imbricates of the Meade thrust were described by Protzman & Mitra (1990, figs. 6–8). Here we report results extending the strain study into the main body of the Meade thrust sheet and into different stratigraphic horizons within the sheet.

Finite strain has been measured throughout the study area using deformed ooids and deformed *Pentacrinus* ossicles. *Pentacrinus* ossicles are found at multiple stratigraphic levels in the Jurassic Twin Creek and Triassic Thaynes Formations. Strain is determined from *camera lucida* drawings of hand samples and direct measurements from thin sections. A finite strain Mohr circle is constructed for each *Pentacrinus* ossicle following the method outlined by Protzman & Mitra (1990).

The tabular nature of crinoid ossicles limits their usefulness in determining three-dimensional strain. Most of the ossicles are disarticulated and tend to lie parallel to the bedding plane. This prevents this strain marker being used for determining strain in the cross-section plane except under special circumstances (Protzman 1985). For this study only bed-parallel crinoid ossicles are used. Yet, as will be shown later, the bedding plane strain data provide an important constraint on the deformation process.

Figure 3 shows the bedding plane strain data for the major imbricate sheets projected on a map. Two populations of bedding plane strain ellipses can be distinguished on the map. The first population of ellipses are seen in the thrust slice containing the upright section of the lower and middle Thaynes Formation. Here the long axis of the bedding plane strain ellipses are parallel to the strike of the beds, and approximately perpendicular to the transport direction. Such orientations are best explained as a result of layer-parallel shortening (LPS). Other workers have recognized LPS fabrics in the Idaho–Wyoming–Utah thrust belt, using markers such as calcite twinning (Allmendinger 1982, Evans & Craddock 1985), cleavage (Mitra & Yonkee 1985) and crinoids (McNaught 1990, Protzman & Mitra 1990).

The second population of strain ellipses is found on the overturned section of the Twin Creek Formation in the easternmost thrust slice (Fig. 3). This population is more variable, with some ellipses oriented with their long axes perpendicular to strike (i.e. parallel to the transport direction). Strain ellipses with strike parallel long axes are best explained as a result of LPS, as argued

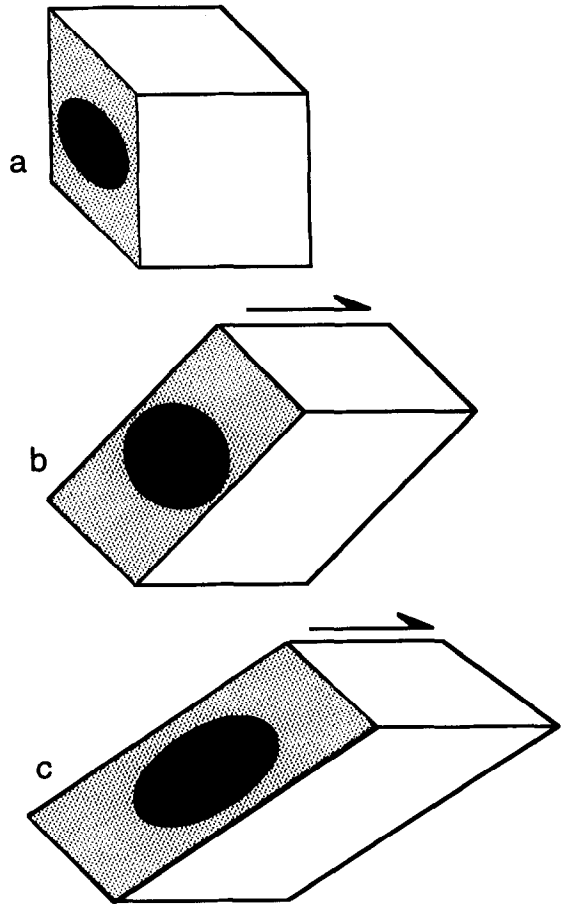


Fig. 4. Cube represents rock undergoing simple shear above a horizontal fault. Base of cube is shear plane. Shaded side is bedding plane, which is not parallel to shear plane. (a) Pre-shear, elliptical strain marker on bedding plane, long axis of ellipse is parallel to strike of bed, consistant with folded layer-parallel shortening (LPS) fabric. (b) Shear stretches short axis of strain ellipse in (a), forming a circular strain marker as bedding plane rotates toward shear direction. (c) Increased shear causes more stretching of the strain marker parallel to the dip of the bed. The long axis of the bedding-parallel strain ellipse points in shear direction.

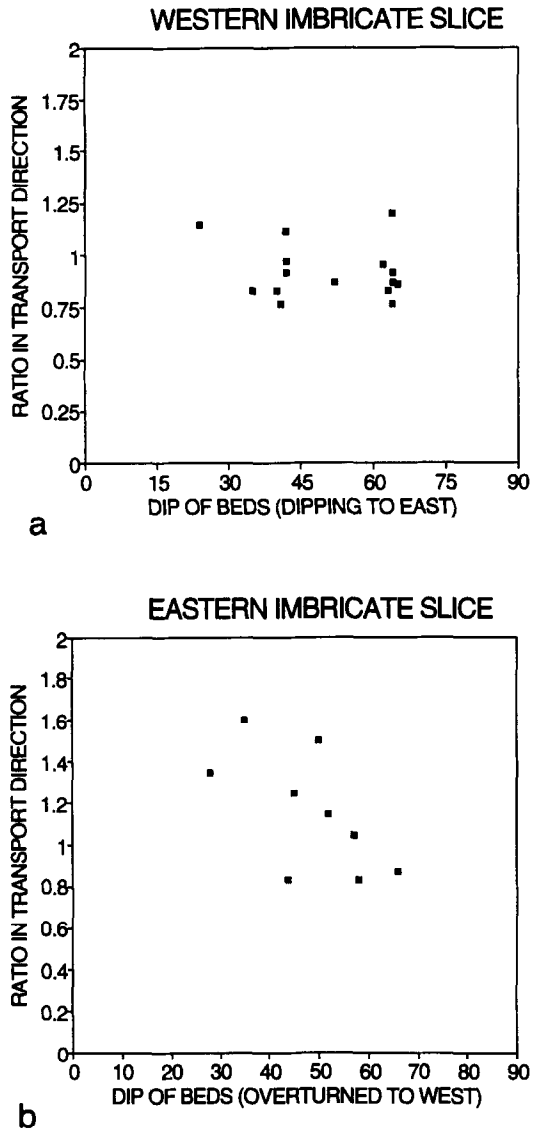


Fig. 5. Plot of axial ratio of bedding plane strain ellipse vs dip of bed. (a) Western imbricate slice (upright section) and (b) eastern imbricate slice (overturned section).

earlier. The origin of ellipses with transport-parallel long axes can be best explained as a result fault-parallel shear. The explanation and the results are consistent with earlier interpretation of fault parallel shear based on cleavage and bedding relationships (Protzman & Mitra 1990). Cleavage rotation is opposite in sense expected for flexural-slip on the limb of the large fold, and the sense of rotation is consistent, precluding rotation owing to flexural-slip associated with folding above small imbricate faults. During shear a spherical marker will develop a long axis that will rotate toward the shear direction. The trace of this ellipsoid on the bedding plane will also elongate toward the shear direction.

Consider an LPS strain fabric represented by a bedding-parallel elliptical marker on the face of a cube. Folding rotates bedding so it is steeply dipping relative to the horizontal shear plane, and perpendicular to the shear direction (Fig. 4a). With progressive shear the marker first becomes less elliptical (Fig. 4b), passes through a circular stage, and eventually becomes elliptical with long axis perpendicular to strike (Fig. 4c). At the same time, the angle between bedding and the shear plane decreases.

The dual orientations of strain ellipses on the bedding planes are not the result of layer-parallel shortening and fault-parallel shear acting separately on different parts of the area but can be explained as a result of inhomogeneous fault-parallel shear modifying original LPS ellipses on bedding. To facilitate comparison of the two populations of ellipses, we normalize the axial ratios by assuming that the strike parallel magnitude of bedding plane strain (stretch) is 1, essentially assuming plane strain. Ellipses whose long axes are perpendicular to strike are thus extensional (axial ratio $>1$) and those whose long axes are parallel to strike are contractional (axial ratio $<1$). These normalized axial ratios of the bedding plane ellipse are plotted against the dip of the bed on which they are found (Fig. 5). In the western slice which includes the upright Lower Thaynes section (Fig. 3), normalized axial ratios vary from 0.8 to 1.1 with no apparent correlation with dip (Fig. 5a). For the overturned Twin Creek section within the easternmost thrust

Table 1. Calculating pre-shear orientation of two stratigraphic units based on changes in thickness

| | Post-shear bed–fault angle ($\theta'$)* (°) | Post-shear bed thickness ($t'$)* (m) | Pre-shear bed thickness ($t_0$)† (m) | Pre-shear fault bed angle ($\theta$)‡ (°) |
|---|---|---|---|---|
| Leeds Creek Member, Twin Creek Formation | 30 | 300 | 500 | 56 |
| Nugget Sandstone | 20 | 200 | 500 | 59 |

*Determined from geological mapping in the hanging wall.
†Determined from geological mapping of corresponding footwall cutoffs.
‡Calculated: $\theta = \sin^{-1}[(t_0/t')\sin(\theta')]$. Modified from Protzman & Mitra (1990).

slice, axial ratios are more variable, ranging from 0.8 up to 1.6 (Fig. 5b).

It is significant that this variation appears to have a crude correlation with dip. The more overturned (gentler dipping) beds show the highest strain axial ratios suggesting that the dip of the overturned beds is also controlled by fault-parallel shear. The least overturned beds (60°) show strain axial ratios similar to the western slice. This indicates that initially both sets of rocks underwent similar LPS. Folding presumably related to movement on the Meade thrust followed, forming an anticline with an overturned forelimb dipping 60° to the west without significant change in the bedding plane strain axial ratio. Finally the forelimb was inhomogeneously sheared, modifying the bedding plane strain axial ratio and dip of the beds.

As mentioned above, beds in the overturned section in the hanging wall of the Meade thrust are significantly thinned compared to the corresponding beds in the footwall exposed to the west. This is further evidence for fault parallel shear. Assuming simple shear parallel to the fault, it is possible to calculate the amount of shear needed to return the thinned beds back to their unsheared thickness (Protzman & Mitra 1990). In addition, the pre-shear orientation of these beds can also be calculated. By unshearing both the Leeds Creek Member of the Twin Creek Formation and the Nugget Sandstone a similar pre-shear orientation (approximately overturned 60° dipping to the west) is found (Table 1). This shows that two different lithologies, in different parts of the sheet, which have been affected by different amounts of shear, both started out with very similar pre-shear orientations. Further, this orientation agrees with what is expected for pre-shear orientation of bedding based on analysis of bedding plane strain ellipses discussed earlier.

Three-dimensional strain data from oolites should be very useful in retrodeforming a cross-section. Limitations, however, are imposed by the limited stratigraphic distribution of oolitic horizons. On a Flinn Diagram (Fig. 6a), the axial ratios of the finite strain ellipsoids for the deformed oolites shows the variation in ellipsoid shape, from prolate to triaxial plane strain. From a stereogram showing the relative orientations of strain ellipsoids with respect to bedding (Fig. 6b) we see that the short axis of the finite strain ellipsoid ($e_3$) is generally at a high angle to bedding, while the flattening plane of the finite strain ellipsoid is at an acute angle to bedding. This may be the result of the bedding plane and the flattening plane converging during fault-parallel shear, or it may be the result of an early sedimentary compaction fabric. The non-oblate nature of the strain ellipsoid (Fig. 6a) indicates that it is probably a result of tectonic deformation rather than compaction. A significant component of compaction strain may also be present.

In summary, the results of the strain analysis indicate that most of the stratigraphic levels that have strain

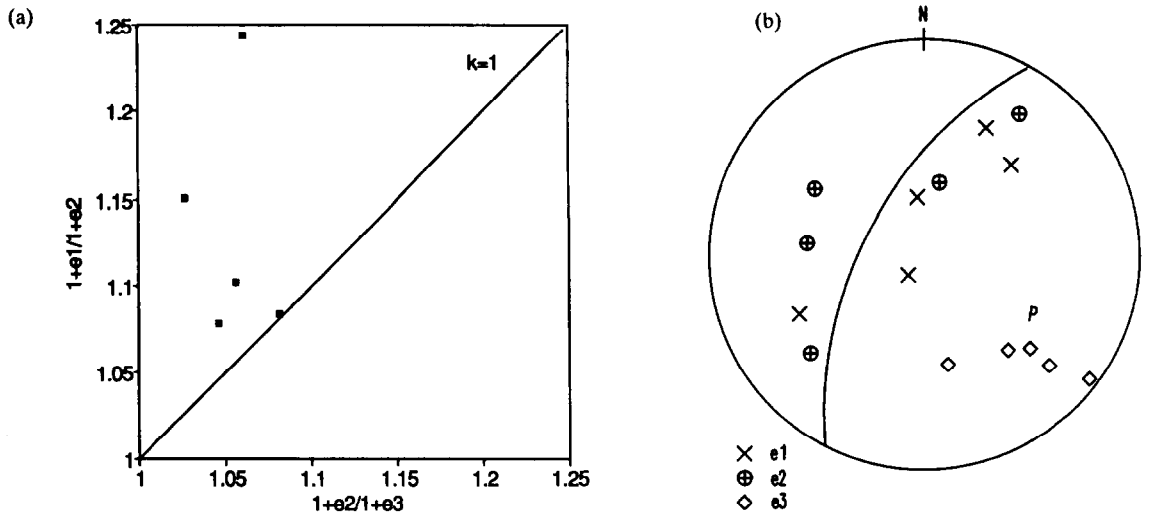


Fig. 6. Strain data for deformed ooliths. (a) Flinn plot. (b) Stereoplot of $e_1$, $e_2$, $e_3$, the directions of long, intermediate and short axes of the strain ellipsoid, respectively. Approximate trace of bedding shown by great circle and pole (p).

markers (Twin Creek and Thaynes Formations) show an early LPS increment of deformation. This is followed by folding which results in overturning of some sections to dips of 60°, but does not affect the bedding plane strain ellipse nor the cleavage–bedding angle. The larger-scale geometry of the folds and faults and the truncation of the faults (Protzman & Mitra 1990, Coogan & Royse 1990) suggest that faulting accompanies folding and most of the folds form as detachment folds or fault propagation folds (McNaught & Mitra 1993). In some fault slices these two early structural styles are modified by a late increment of fault-parallel shear. While these are the components of deformation that can be recognized from field data, there may be other components which are compatible with this data and may be recognized as a result of the retrodeformation process during section balancing, such as additional components of shear or compaction.

## RETRODEFORMING THE MEADE THRUST

The two essential starting components of the retrodeformation process have been developed earlier. The first is a cross-section, including strain data. The second is the deformational model, which is not necessarily the same across the whole section (i.e. different parts of the section may have followed different deformation paths). Both the model and the cross-section consist of constrained and unconstrained portions. The constrained portions are fixed by data, whereas the unconstrained portions are based on interpretation. The constrained portion of the cross-section is determined by surface data, the unconstrained portion is our interpretation of the subsurface. The constrained portion of the deformation model consists of the steps necessary to explain the observed structures and strain patterns. The unconstrained portions of the deformational model are the additional steps necessary to go from the undeformed to the deformed states. It is the unconstrained portions of either the deformation model or the cross-section that need to be altered in order to produce a retrodeformable section.

The deformation model used here is based on all hanging wall and footwall information available to date, and has differences in detail from that used by Protzman & Mitra (1990) which was based mainly on data from the footwall and frontal hanging wall slice. The first step in retrodeforming this section is to pull the thrust sheet back (Fig. 7a) so that the frontal slice is returned to its footwall cut-off (Fig. 7b). In doing so folding is removed from the footwall and small thrust slices are also restored. The second step is to remove fault parallel shear from the overturned section. This is done by unshearing parallel to the upper flat and removing the amount of shear that will bring the overturned beds back to a 60° overturned dip, consistent with footwall dips. At the same time the section-parallel strain ellipses calculated from deformed oolites (Fig. 8a) are also unsheared (Fig. 8b). Unshearing also returns the present cleavage–bedding angle (52°) to 75° (Fig. 9) rather than 90° expected for LPS. This presents a problem in continuing the retrodeformation process, since none of the remaining steps in our model (such as folding or LPS) will alter the cleavage–bedding angle. If we continue unshearing (Fig. 10) it is clear that the cleavage–bedding angle will start to decrease after reaching a maximum (75°). Thus our first retrodeformation step returns the cleavage–bedding angle to its maximum possible value.

Because the next steps will not alter this cleavage–bedding angle, we need to change either the unconstrained portion of our deformation model or the unconstrained portion of our cross-section in order to continue to retrodeform this section. Since the problem lies in a constrained portion of the section (we know the cleavage–bedding angle and bed-fault angle), it is the deformation model that we need to modify. We could modify our model in a number of different ways. The most likely solution is a new increment of fault-parallel shear in a new orientation. This new direction is most likely related to the cutting out of the upright limb of the anticline. This step in the restoration is different from Protzman & Mitra (1990), which proposed a one-step fault-parallel shear restoration and did not quantify this second increment of fault-parallel shear.

This new direction can be found by considering the effect of a new shear direction on the cleavage–bedding angle (Fig. 10). It can be seen that in order to obtain a cleavage–bedding angle of 90° it is necessary to have the shear direction inclined at least 30° to the footwall flat. An additional constraint is provided by the thickness of the beds in the thrust sheet. Since the thickness of the beds after the first component of unshearing approached the thickness observed in the footwall, additional thickening of the beds cannot be allowed. Figure 10 is contoured for percent change in thickness required by unshearing. To keep the thickening to about 5% and to return the cleavage–bedding angle to 90°, it is necessary to have an orientation of shear at 40° to the footwall flat and an angular shear of about 15°.

We are left with a restored anticline (detachment fold) (Fig. 7c), with cleavage now perpendicular to bedding. The new orientation of the strain ellipses in the section are oriented in the sense expected by bed-parallel shear during flexural-slip folding (Fig. 8c). For the next retrodeformation step we unfold the fold, removing differential amounts of bed-parallel shear (ranging from a low of 0° for bed normal cleavage to a high of about 12° for one of the oolitic samples). The result is a layer-cake section where both cleavage and all the strain ellipses have their long axes perpendicular to bedding (Fig. 8d). At the same time the western slice is restored to the ramp of the Meade thrust (Fig. 7d). The final restoration produces an admissible ramp–flat structure unlike the western end of the restored section in Protzman & Mitra (1990, fig. 11 stage 5).

The remaining deformation that needs to be removed is layer-parallel shortening (LPS). The amount of shortening that needs to be removed is indicated by the bed-perpendicular cleavage and the strain ellipses (in oolitic

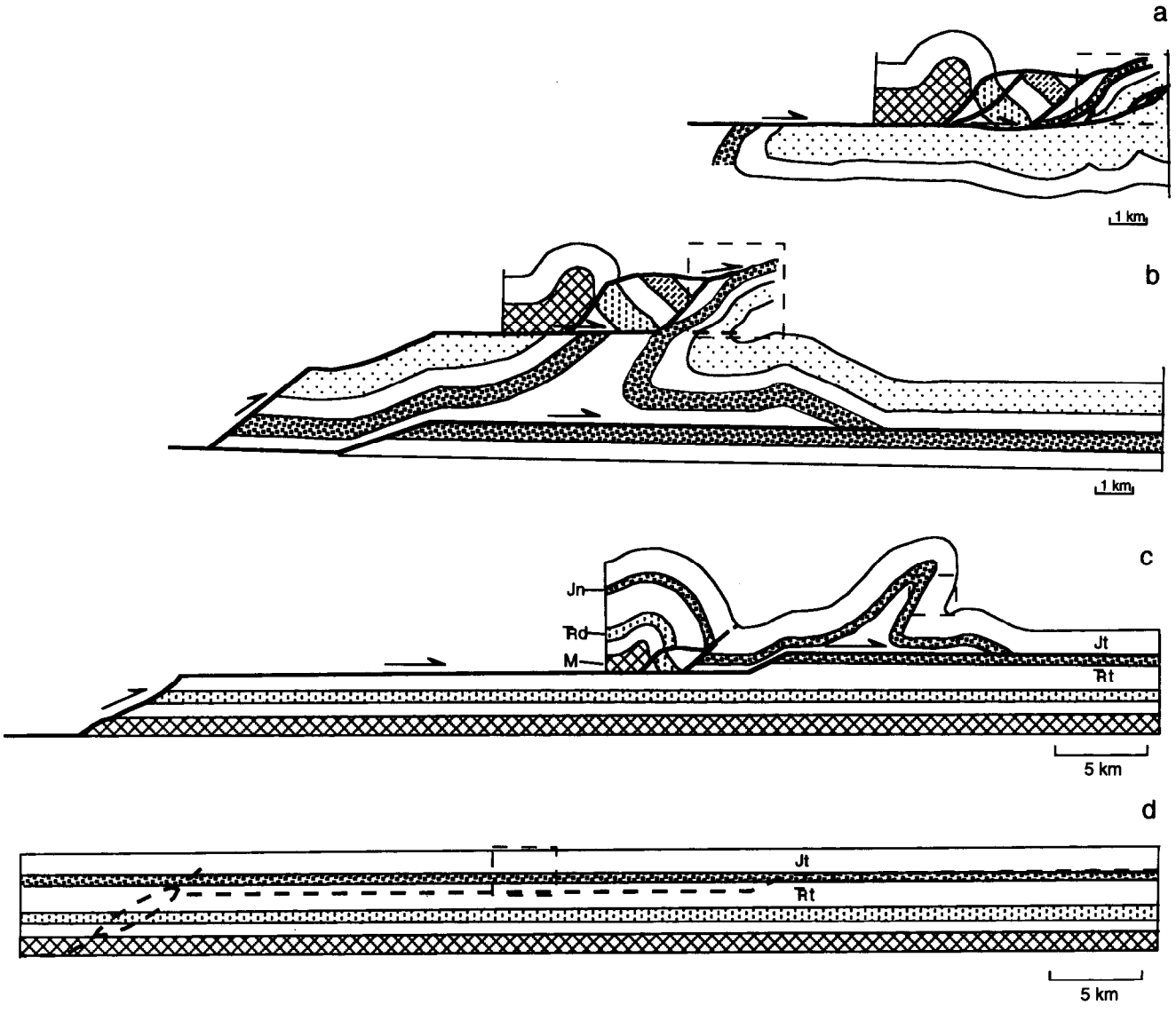


Fig. 7. Retrodeformation sequence for the Meade Peak area (cross-section, Fig. 2). Boxed area is highlighted in Fig. 8. (a) Major folding in footwall removed. (b) Thrust sheet pulled back to its footwall cut-off and additional footwall folding removed. (c) Fault-parallel shear and imbrication removed from leading detachment fold. (d) Remaining part of the thrust sheet pulled back to its footwall cut-offs. Folding and LPS is removed. Note scale change between sections (a) and (b), and sections (c) and (d).

beds) in the plane of section. In three dimension, most of the strain ellipsoids in oolitic beds have their long axes oriented perpendicular to the section plane. The axial ratio in the bedding plane is about 1.1–1.2, which is the same as that calculated above for layer-parallel shortening from the bedding plane strain ellipses in *Pentracrinus*-bearing layers. All of these shortening values are in agreement with the amount of layer parallel shortening calculated for cleavage in the Twin Creek Formation (Mitra & Yonkee 1985).

The final stage in retrodeforming this section is removing ~15% (stretch = 0.85) LPS from the section, that is lengthening the section by ~18% (stretch = 1/0.85 = 1.18). There are two ways in which this can be done. One is to assume constant area, which results in thinning each bed by ~15%. This has been suggested by Protzman & Mitra (1990), based on the presence of coeval veins and pressure solution seams perpendicular to the plane of section. The second is by area loss or gain. This results in lengthening of the section by ~18% without changing bed thicknesses. This extra material either moved out of the section (non-plane strain) or moved out of the system entirely (volume-loss strain). The presence of calcite veins that generally form parallel to the section, and could be the sink of the material lost from pressure solution seams, suggests a component of non-plane strain. The truth probably lies somewhere in between, with some thickening and some out-of-plane strain during the early increment of LPS fabric development.

## DISCUSSION

Initially it may seem that the main reason for incorporating strain data into a balanced cross-section is to adjust bed lengths and/or areas in order to produce a restored section or to determine the amount of shorten-

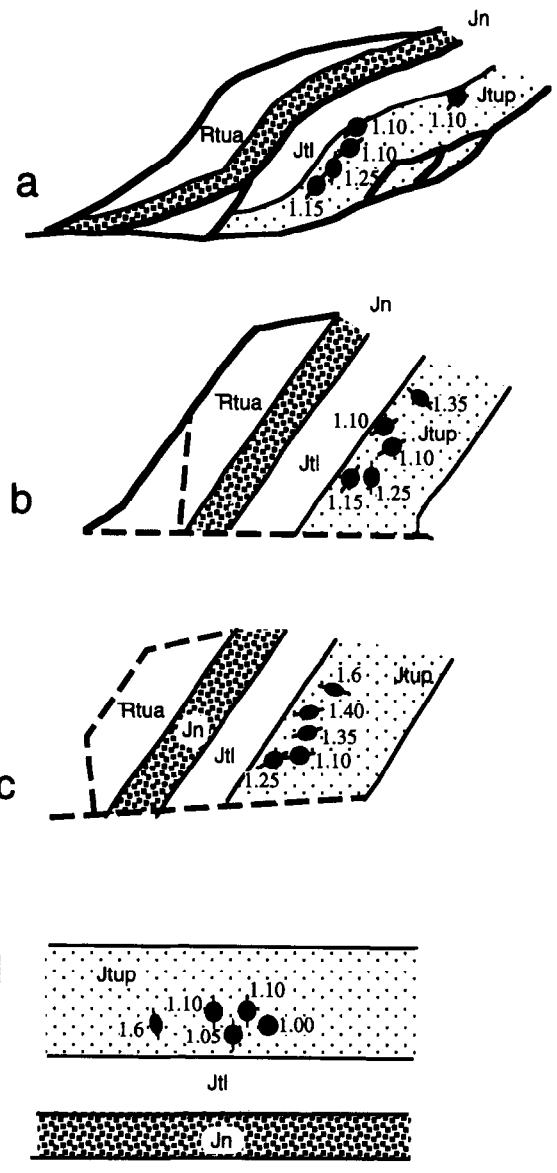


Fig. 8. Retrodeformation of section-parallel finite strain ellipse determined from deformed oolites. Box on Fig. 7 shows location of this part of the section during retrodeformation. (a) Deformed section. (b) After removing main component of fault-parallel shear. (c) After removing second component of fault-parallel shear. (d) After removing folding and differential flexural-slip.

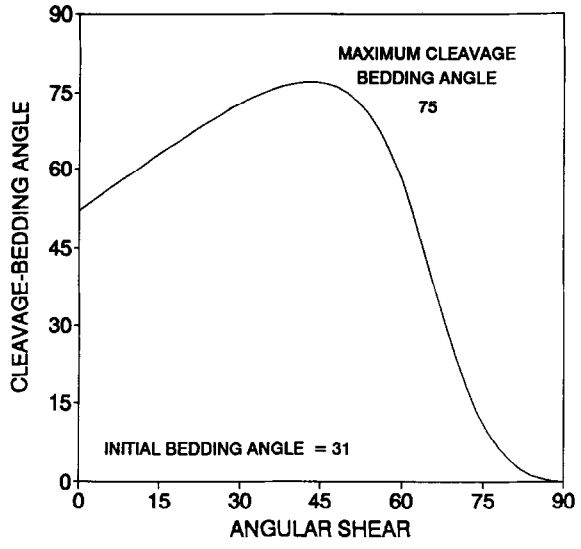


Fig. 9. Change in cleavage–bedding angle for progressive removal of angular shear. Initial bed fault angle is 31° and cleavage–bedding angle is 52°. Maximum possible cleavage–bedding angle is 75°.

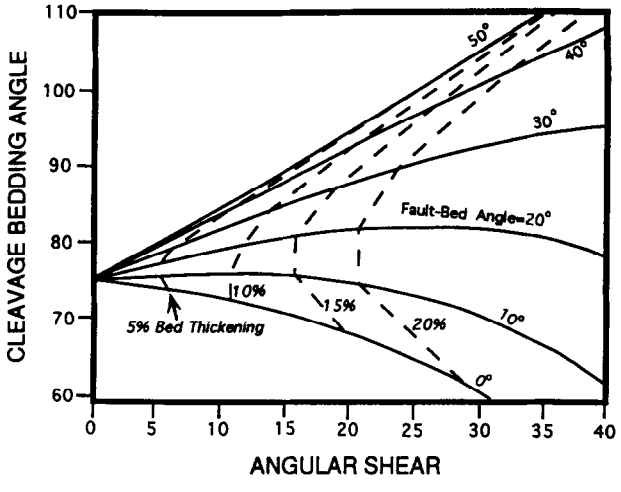


Fig. 10. Change in cleavage–bedding angle for progressive removal of angular shear. Initial cleavage–bedding angle is 75°. Curves drawn for fault-bed angles of 60, 50, 40, 30. 20 and 10° (corresponding to fault dips of 0, 10, 20, 30, 40 and 50°).

ing in the section (Woodward *et al.* 1986, Ford 1987). In theory this is the only correct way for an internally deformed thrust sheet to be restored, because if the strain is not removed holes will develop in the restored section. In practice, as can be seen earlier, the missing area can just as easily be accommodated by changing the geometry of the unconstrained portion of the deformed section and ignoring the internal deformation.

Failure to incorporate strain data into a section may give the false impression of a balanced section. If strain data are included there will still be portions of the section for which no data are available, either because of the limited distribution of strain markers or because of locations that are impossible to sample (eroded or subsurface). The lack of strain data from all parts of a section makes it impossible to show that all deformation has been accounted for.

Rather than trying to calculate shortening or area change from our strain data we chose to treat it like other geometric data. Just as a folded bed in the deformed section must be returned to a layer-cake geometry in the restored section, strain ellipsoids and strain ellipses must restore to spheres and circles. One of the advantages of this approach is that bedding plane strain ellipses, which are most common, can be incorporated into the section.

In the earlier analysis a model is developed for deformation associated with the emplacement of the Meade thrust sheet and a constrained cross-section has been constructed. The advantage of the retrodeformation process presented is that it requires that the section and the deformation model complement each other, i.e. each is used to constrain the other. Not only then is the section geometrically possible but the deformation path is also physically possible. The linking of the model and section means that a retrodeformable section on its own

is meaningless unless the corresponding deformation model is also presented. Further, a retrodeformable section and an associated model may represent only one of many possible solutions. The number of possibilities can only be restricted if sufficient data are available.

The development of the deformation model is probably the most difficult step in the process. While incremental strain markers would greatly assist this process, the model presented illustrates how careful study of finite strain markers and the orientation of mesoscopic structures, such as cleavage, can be used to determine a possible deformation history. Even strain ellipses which do not lie parallel to the section plane can be used in developing the deformational model. This approach allows for the straightforward incorporation of a variety of detailed structural data such as geological maps, seismic sections, well logs, incremental strain, three-dimensional finite strain, two-dimensional finite strain, and the orientation of mesoscopic features such as cleavage and slickensides.

The method described here not only allows restorations of complex structures using a simple step-by-step approach based on geological history, but also ensures that no physically impossible configurations were reached during the inferred structural evolution. This is particularly important in the internal portions of fold–thrust belts where the complex structures are difficult to restore to their undeformed state, and erroneous conclusions might be reached if a simple, one-step restoration was attempted.

## CONCLUSION

The Meade Peak and Georgetown Canyon areas formed as a result of the Meade thrust truncating a preexisting anticline developed out in front of the propagating thrust. Penetrative deformation within these areas is primarily the result of layer-parallel shortening. Locally additional fault-parallel shear strain developed during thrusting.

Successful retrodeformation of the section through the Meade Peak area is achieved first by pulling the thrust sheet back and removing fault-parallel shear, second, by unfolding and removing heterogeneous flexural-flow and, finally, by removing layer-parallel shortening.

Both two- and three-dimensional strain data can be incorporated into cross-sections by developing a model that is used to retrodeform both the section and the strain data. While a unique solution will not be possible in most cases, finite strain data provides additional constraints on section geometry.

*Acknowledgements*—This work was supported by NSF grant EAR-8916629 to G. Mitra and grants from the Geological Society of America, Sigma Xi and the American Association of Petroleum Geologists to M. McNaught. We thank T. Apotria and S. Treagus for reviews of this manuscript, and M. Ford, R. Allmendinger and an anonymous reviewer for comments on an earlier version.

## REFERENCES

Allmendinger, R. W. 1981. Structural geometry of the Meade thrust plate in northern Blackfoot Mountains, southeastern Idaho. *Bull. Am. Ass. Petrol. Geol.* **65**, 509–525.

Allmendinger, R. W. 1982. Analysis of microstructures in the Meade plate of the Idaho–Wyoming foreland thrust belt, U.S.A. *Tectonophysics* **85**, 221–251.

Armstrong, F. C. & Cressman E. R. 1963. The Bannock thrust zone, southeastern Idaho. *Prof. Pap. U.S. Geol. Surv.* **374J**.

Armstrong, F. C. & Oriel, S. S. 1965. Tectonic development of the Idaho–Wyoming thrust belt. *Bull. Am. Ass. Petrol. Geol.* **49**, 1847–1866.

Blackstone, D. L. & DeBruin, R. H. 1987. Tectonic map of the overthrust belt, western Wyoming, northeastern Utah and southeastern Idaho. *Geol. Surv. Wyoming Map Ser.* 23.

Borden, R. K. 1986. Structural geology and stratigraphy of the southwestern margin of the Meade thrust sheet, Harrington Peak, Georgetown and Meade Peak quadrangles, southeastern Idaho. Unpublished masters thesis, South Dakota School of Mines and Technology.

Burgel, W. D., Rodgers, D. W. & Link, P. K. 1987. Mesozoic and Cenozoic structures of the Pocatello region, southeastern Idaho. In: *Wyoming Geological Association Guidebook* (edited by Miller, W. R.). Wyoming Geological Association, 91–100.

Coogan, J. C. & Royse, F. 1990. Overview of recent developments in thrust belt interpretation. In: *Geologic Field Tours of Western Wyoming and Parts of Adjacent Idaho, Montana and Utah* (edited by Roberts, S.), 89–126.

Coogan, J. C. & Yonkee, W. A. 1985. Salt detachments in the Jurassic Preuss redbeds within the Meade and Crawford thrust systems, Idaho and Wyoming. In: *Orogenic and Stratigraphic Patterns of North-central Utah and Southeastern Idaho.* Utah Geol. Ass. Publ. 14.

Cressman, E. R. 1964. Geology of the Georgetown Canyon–Snowdrift Mountain area, southeastern Idaho. *Bull. U.S. geol. Surv.* **1153**.

Dahlstrom, C. D. A. 1970. Structural geology in the eastern margin of the Canadian Rocky Mountains. *Bull. Can. Petrol. Geol.* **18**, 332–406.

DeCelles, P. G. 1988. Lithologic provenance modeling applied to the Late Cretaceous synorogenic Echo Canyon Conglomerate, Utah: a case of multiple source area. *Geology* **16**, 1039–1043.

DeCelles, P. G. 1994. Late Cretaceous-Paleocene synorogenic sedimentation and kinematic history of the Sevier thrust belt, northeast Utah and southwest Wyoming. *Bull. Geol. Soc. Am.* **106**, 32–56.

DeCelles, P. G., Pile, H. T. & Coogan, J. C. 1993. Kinematic history of the Meade thrust based on provenance of the Bechler Conglomerate at Red Mountain, Idaho, Sewier thrust belt. *Tectonics* **12**, 1436–1450.

Dixon, J. S. 1982. Regional structural synthesis, Wyoming salient of the western overthrust belt. *Bull. Am. Ass. Petrol. Geol.* **10**, 1560–1580.

Dover, J. H. 1985. Geologic map and structure sections of the Logan 30′ × 60′ quadrangle Utah and Wyoming. *U.S. Geol. Surv. Open-file Rep.* **85-216**.

Elliott, D. 1983. The construction of balanced cross-sections. *J. Struct. Geol.* **5**, 101.

Evans, J. P. & Craddock, J. P. 1985. Deformation history and displacement transfer between the Crawford and the Meade thrust systems, Idaho–Wyoming overthrust belt. In: *Orogenic and Stratigraphic Patterns of North-central Utah and Southeastern Idaho.* Utah Geol. Ass. Publ. 14.

Ford, M. 1987. Practical application of the sequential balancing technique: an example from the Irish Variscides. *J. geol. Soc. Lond.* **144**, 885–891.

Heller, P. L., Bowdler, S. S., Chambers, H. P., Coogan, J. C., Hagen, E. S., Shuster, M. W., Winslow, N. S. & Lawton, T. F. 1986. Time of initial thrusting in the Sevier orogenic belt, Idaho–Wyoming–Utah. *Geology* **14**, 388–391.

Lamerson, P. R. 1982. The fossil basin and its relationship to the Absaroka thrust system, Wyoming and Utah. In: *Geologic Studies of the Cordilleran Thrust Belt* (edited by Powers, R. B.). Rocky Mountain Association of Geologists Symposium, 279–340.

Mansfield, G. R. 1927. Geography, geology, and mineral resources of part of southeastern Idaho. *Prof. Pap. U.S. geol. Surv.* **152**.

McNaught, M. A. 1990. The use of retrodeformable cross sections to constrain the geometry and interpret the deformation of the Meade

thrust sheet, southeastern Idaho and northern Utah. Unpublished Ph.D. thesis, University of Rochester.

McNaught, M. A. & Mitra, G. 1993. A kinematic model for the origin of footwall synclines. *J. Struct. Geol.* **15**, 805–808.

Mitra, G., Hull, J. M., Yonkee, W. A. & Protzman, G. M. 1988. Comparison of mesoscopic and microscopic deformation styles in the Idaho–Wyoming thrust belt and the Rocky Mountain foreland. In: *Interaction of the Rocky Mountain Foreland and the Cordilleran Thrust Belt* (edited by Schmitt, C. J. & Pery, W. J.). *Mem. geol. Soc. Am.* **171**, 119–141.

Mitra, G. & Yonkee, W. A. 1985. Relationship of spaced cleavage to folds and thrusts in the Idaho–Utah–Wyoming thrust belt. *J. Struct. Geol.* **7**, 361–373.

Mitra, G., Yonkee, W. A. & Gentry, D. J. 1984. Solution cleavage and its relationship to major structures in the Idaho–Utah–Wyoming thrust belt. *Geology* **12**, 354–358.

Oriel, S. S. & Armstrong, F. C. 1966. Times of thrusting in the Idaho–Wyoming thrust belt: Reply. *Bull. Am. Ass. Petrol. Geol.* **50**, 2614–2621.

Protzman, G. M. 1985. The emplacement and deformation history of the Meade thrust sheet, southeast Idaho. Unpublished Masters thesis, University of Rochester.

Protzman, G. M. & Mitra, G. 1990. Strain fabric associated with the Meade thrust sheet: implications for cross-section balancing. *J. Struct. Geol.* **12**, 403–417.

Royse, F., Warner, M. A. & Reese, D. L. 1975. Thrust belt structural geometry and related stratigraphic problems, Wyoming–Idaho–northern Utah. In: *Rocky Mountain Association of Geologists Symposium*, 41–54.

Valenti, G. L. 1982. Structure of the Laketown quadrangle and petroleum exploration in the Bear Lake area, Rich country, Utah. In: *Geologic Studies of the Cordillerian Thrust Belt* (edited by Powers, R. B.). Rocky Mountain Association of Geologists, 859–868.

Wiltschko, D. V. & Dorr, J. A., Jr 1983. Timing of deformation in overthrust belt and foreland of Idaho, Wyoming, and Utah. *Bull. Am. Ass. Petrol. Geol.* **67**, 1304–1322.

Woodward, N. B., Boyer, S. E. & Suppe, J. 1985. *An Outline of Balanced Cross Sections. Studies in Geology*, Vol. II (2nd edn). University of Tennessee Department of Geological Sciences.

Woodward, N. B.,, Gray, D. R. & Spears, D. B. 1986. Including strain data in balanced cross sections. *J. Struct. Geol.* **8**, 313–24.

sg 18:5-D